Nuclear Physics B251[FS13] (1985) 353–373

DEFINITION AND STATISTICAL PROPERTIES OF A UNIVERSAL TOPOLOGICAL CHARGE

B. BERG

II. Institut für Theoretische Physik, Luruper Chaussee 149, D-2000 Hamburg 50, West Germany

C. PANAGIOTAKOPOULOS

Physics Department, Rockefeller University, 1230 York Avenue, New York, NY 10021-6399, USA

Received 30 April 1984

We consider the 2d O(3) σ-model. Lattice topological charge and universality are reconciled by an appropriate (quasi) *local* definition of the topological charge. Numerical calculations are carried out on square and triangular lattices. The results are satisfactory within limitations coming from the Monte Carlo method.

1. Introduction

For 2d CP^N models and 4d non-abelian gauge theories a topological charge separates the classical fields into various topological sectors. Within the semi-classical expansion quantities related to the topological charge can be investigated, and topology has been argued to be important in the pattern of chiral symmetry breaking [1]. The role of topology on the quantum level is, however, not well understood, because fields contributing to the Feynman path integral are typically discontinuous on a physical scale [2]. This means that within the lattice regularization one has to impose a certain notion of continuity on the scale of one lattice spacing in order to insure that topological sectors exist in the continuum limit.

In the case of the 2d CP^N models a lattice topological charge was introduced in ref. [3]. For simplicity we will mainly consider the 2d O(3) σ-model (CP^1 model) in this article*. For this model the topological charge of ref. [3] amounts to dividing the lattice into triangles and to summing up the signed minimal areas of the spherical triangles, which are spanned on S_2 by the spin vectors. The following properties are

* Generalization to the CP^N models is straightforward.

important:

(i) The topological charge takes integer values and sums up from a *local* charge density:

$$Q = \sum_{\mathrm{p}} q(\mathrm{p}) = 0, \pm 1, \pm 2, \ldots . \tag{1.1}$$

Here the sum goes over all plaquettes (squares or triangles) of the 2d lattice considered (periodic boundary conditions are assumed).

(ii) The classical continuum charge density $q_{\mathrm{cl}}(x)$ [4] is obtained in the classical continuum limit

$$\lim_{a \to 0} q(\mathrm{p}) = q_{\mathrm{cl}}(x_{\mathrm{p}}) \tag{1.2}$$

(x_{p} is the coordinate of the centre of the plaquette p).

(iii) The topological charge Q is defined (by (1.1)) up to configurations which are of measure zero in the functional integral. These configurations are called *exceptional* and there exists a fixed $\varepsilon_0 > 0$ such that for any exceptional configuration there exists at least one link ℓ with $S_\ell \geqslant \varepsilon_0$. S_ℓ is the action of link ℓ (normalized to $\lim_{\beta \to \infty} \langle S_\ell \rangle = 0$).

From (1.2) it follows that $\delta Q = 0$ for an infinitesimal variation δ of the spin fields. Varying fields continuously the topological charge can only change by passing through an exceptional configuration. The lattice topological charge Q separates field configurations on a finite periodic lattice into sectors of integer charge and the exceptional configurations form the boundaries between topological sectors in the lattice theory.

In weak coupling perturbation theory one considers small fluctuations around a constant field. Consequently, with the above properties of the lattice topological charge, the topological susceptibility

$$\chi_{\mathrm{t}} = \lim_{V \to \infty} \frac{1}{V} \langle Q^2 \rangle \tag{1.3}$$

vanishes to all orders of weak coupling perturbation theory. By dimensional arguments χ_{t} is therefore expected to scale with the dimension of $[m^2]$, m being a physical mass. This means

$$\chi_{\mathrm{t}} = a^{-2} \mathrm{const}_{\mathrm{t}} \exp(-4\pi\beta)(1 + \mathrm{O}(1/\beta)), \qquad \beta \to \infty . \tag{1.4}$$

The O(3) σ-model is, however, a special case, because the power law of eq. (1.4) may be modified by the ultraviolet divergence [5] of the instanton scale size integration and the continuum limit of the topological susceptibility may not exist. For exploratory Monte Carlo (MC) studies the problem is of minor importance, as the MC data are not sensitive to the power law behaviour.

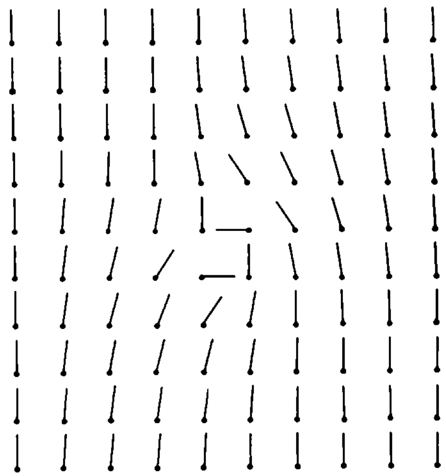

Fig. 1. Minimal action spin configuration [7] in the neighbourhood of the sector $|Q| = 1$.

The first MC calculations were carried out in ref. [3] and the scaling law (1.4) failed completely. In subsequent papers [6–8] the wrong scaling behaviour of the topological susceptibility was diagnosed to be due to short-range fluctuations of the topological charge, called "*dislocations*" in ref. [6], with such a small action that they overwhelm the contribution of slowly varying fields. Due to Lüscher [7] the minimal action of a dislocation of topological charge $|Q| = 1$ is given by

$$S_{\mathrm{D}} = 6.69\ldots, \tag{1.5}$$

corresponding to the spin configuration of fig. 1. The configuration itself is exceptional, but in any neighbourhood unexceptional configurations of charge $|Q| = 1$ are found.

We delegate a preciser discussion to sect. 3 and adapt first a heuristic picture: on the lattice dislocations are local maxima of the action and therefore very different from instantons [4], for which the action is a local minimum everywhere*. For $\beta \to \infty$ dislocations become dilute (in units of the lattice spacing a) and their contribution to the topological susceptibility behaves as

$$\chi_{\mathrm{d}} = a^{-2}\mathrm{const}_{\mathrm{d}}\beta^{p'}\exp(-\beta S_{\mathrm{d}}) \quad \text{for } \beta \to \infty\,. \tag{1.6}$$

As $S_{\mathrm{d}} < 4\pi$ in the O(3) σ-model, dislocations give for large β the dominant contribution to the topological susceptibility (using the above definition [3] for the topological charge). They are non-universal short-distance fluctuations and their

* Due to the breaking of scale invariance instanton-like configurations do not exist in the lattice O(3) σ-model [6, 7] (with the standard action).

contribution to the topological susceptibility has to be regarded as an unphysical infinity. There are similarities to renormalization: we have an infinite unphysical contribution to the topological charge, which has to be subtracted. But the infinite contribution vanishes to all orders of perturbation theory, and no normalization conditions can be formulated to extract the physical finite part. Presently this is the only example of a non-perturbative infinity. Several attempts have been made to cure the problem.

In ref. [6] a heuristic definition for a physical background charge Q_{B} was used and within large statistical errors MC data for the corresponding background susceptibility were consistent with scaling (1.4). Lüscher [7] recognized that in the CP^{N} models with $N \geqslant 2$ appropriate actions (for $N \geqslant 3$ for instance the standard actions) exist, such that the contribution of the short-range fluctuations no longer dominates the physical contributions. A decisive disadvantage remains: no prescription is given which is conjectured to give the same (physical) topological susceptibility on all different actions of the whole universality class. Should we blame the action or the definition of the topological charge, if unphysical results are obtained? Universality is no longer manifestly formulated. (All actions with identical classical continuum limits are supposed to be in the same universality class, for a review see [9].)

Martinelli et al. [8] tried to remedy the situation by introducing a *non-local* definition of the lattice topological charge. Their "block topological" charge suffers, however, from kinematical ultraviolet divergencies [10]. The authors of ref. [8] propose then a regularized definition, but it is not obvious to what extent the continuum limit is expected to be uniquely defined.

One of the present authors [11] proposed a (quasi) *local* universal definition of the topological charge. Roughly speaking it amounts to dividing the previous [3] charge Q into

$$Q = Q_{\mathrm{B}} + Q_{\mathrm{D}}, \tag{1.7}$$

where Q_{D} is the dislocation charge and Q_{B} the physical background charge. In the case of Lüscher's appropriately chosen actions the dislocation charge vanishes and $Q = Q_{\mathrm{B}}$. In the present paper we elaborate several details and carry out an exploratory MC study. Our MC data for the physical topological background susceptibility $\chi_{\mathrm{B}} = (1/V)\langle Q_{\mathrm{B}}^{2}\rangle$ are consistent with the scaling behaviour (1.4). The computer implementation of the new topological charge requires a number of logical decisions to be made by the computer.

The paper is organized as follows: in sect. 2 basic notation is introduced. The universal definition of the topological charge is given in sect. 3. Details of its computer implementation are contained in sect. 4, where also our MC results are presented. Finally concluding remarks are given in sect. 5.

2. Preliminaries

The (standard) action of the 2d O(3) σ-model is defined by

$$S = \sum_{\ell} S_{\ell}, \qquad S_{\ell} = 1 - s_{i(\ell)} s_{j(\ell)}. \tag{2.1}$$

The sum goes over all links ℓ of the lattice and $i(\ell)$, $j(\ell)$ are the endpoints of link ℓ. Vacuum expectation values are calculated with respect to the partition function

$$Z = \int \prod_j \mathrm{d}s_j \, \mathrm{e}^{-\beta S}. \tag{2.2}$$

The product goes over all sites of the lattice and with $s_j = (\cos\theta_j, \sin\theta_j \sin\phi_j, \sin\theta_j \cos\phi_j)$ the measure is given by

$$\int \mathrm{d}s_j = \frac{1}{4\pi} \int_{-1}^{+1} \mathrm{d}\cos\theta_j \int_0^{2\pi} \mathrm{d}\phi_j. \tag{2.3}$$

In our investigation we will consider square and triangular lattices with periodic boundary conditions. For the triangular lattice our conventions are as in ref. [12]. The lattice is spanned by the unit vectors $\hat{e}_1 = (1,0)$ and $\hat{e}_2 = \left(\frac{1}{2}, \frac{1}{2}\sqrt{3}\right)$, the boundary condition is $P(x) = P(x + L_1\hat{e}_1) = P(x + L_2\hat{e}_2)$, the volume is $V = \frac{1}{2}\sqrt{3}\, L_1 L_2$, and the lattice is approximately square with the choice $L_1 \approx \frac{1}{2}\sqrt{3}\, L_2$.

Let us repeat the definition [3] of the topological charge. We consider first the triangular lattice. To each triangle p three spins are attached. Up to *exceptional configurations*

$$s_1 \cdot (s_2 \times s_3) = 0, \qquad 1 + s_1 \cdot s_2 + s_2 \cdot s_3 + s_3 \cdot s_1 \leqslant 0, \tag{2.4}$$

three spins s_1, s_2, s_3 ($s_i^2 = 1$) on the sphere S_2 define uniquely (by interpolating along the geodesics) a minimal spherical triangle with angles $\alpha_1, \alpha_2, \alpha_3$ and area $A = \alpha_1 + \alpha_2 + \alpha_3 - \pi$. The signed area is $A_\sigma(s_1, s_2, s_3) = \sigma A$, $\sigma = \mathrm{sign}[s_1 \cdot (s_2 \times s_3)]$, and with the definition

$$q(\mathrm{p}) = \frac{1}{4\pi} A_\sigma(s_1, s_2, s_3). \tag{2.5}$$

of the topological charge density, the topological charge $Q = \Sigma_{\mathrm{p}} q(\mathrm{p})$ satisfies the requirements (i)–(iii) of the introduction.

For an exceptional configuration we find at least one link ℓ with $S_\ell \geqslant \varepsilon_0^\Delta$, and from eq. (2.4) we see

$$\varepsilon_0^\Delta = \tfrac{4}{3}. \tag{2.6}$$

On the square lattice there are two equally good definitions of the topological charge, according to the two possibilities of dividing the square p into triangles:

$$q_1(\mathrm{p}) = \frac{1}{4\pi}\{A_\sigma(s_1, s_2, s_4) + A_\sigma(s_3, s_4, s_2)\}, \tag{2.7a}$$

$$q_2(\mathrm{p}) = \frac{1}{4\pi}\{A_\sigma(s_2, s_3, s_1) + A_\sigma(s_4, s_1, s_3)\}. \tag{2.7b}$$

For exceptional configurations at least one link ℓ with $S_\ell \geq \varepsilon_0^\square$ exists, and from eq. (2.4)

$$\varepsilon_0^\square = 1 \tag{2.8}$$

follows. Also, we have for fields with $S_\ell < \varepsilon_0^\square$ (all ℓ) $q_1(\mathrm{p}) = q_2(\mathrm{p})$. Otherwise $q_1(\mathrm{p}) - q_2(\mathrm{p}) = 0, \pm 1$ is possible.

It is instructive to note [8] that in the CP^1 gauge language the topological charge density (2.5) can be defined in close analogy with the discussion of the topological charge in the continuum, and the charge density at a triangle is identical with the fractional part of a surface integral around a triangle. Let us fix the CP^1 gauge, for instance by the requirement $z_1(x)$ real, where x denotes a site of the lattice. Then the $z(x) = (z_1(x), z_2(x))$ field of the CP^1 model is uniquely related to the s-field (2.1) by means of $s^i = \bar{z}_\alpha \sigma^i_{\alpha\beta} \bar{z}_\beta$ (σ^i Pauli matrices), and furthermore

$$u(x, \hat{\mu}) := \frac{\bar{z}(x+\hat{\mu}) z(x)}{|\bar{z}(x+\hat{\mu}) \cdot z(x)|} = \mathrm{e}^{i\phi(x, \hat{\mu})}, \qquad \hat{\mu} \in \{(\pm 1, 0), (0, \pm 1)\}, \tag{2.9}$$

defines uniquely a phase $\phi(x, \hat{\mu}) \in (-\pi, \pi)$*. Let $\mathrm{S} = ((x_1, \hat{\mu}_1), (x_2, \hat{\mu}_2), \ldots, (x_f, \hat{\mu}_f))$ be a closed self-avoiding curve along the links $\ell_i = (x_i, \hat{\mu}_i)$, $(i = 1, \ldots, f)$ of the lattice. S is the "surface" of a connected region. The fractional part $q_\mathrm{F}(\mathrm{S})$ of the surface integral is defined by

$$q_\mathrm{F}(\mathrm{S}) = \frac{1}{2\pi} \arg\left[u(x_1, \hat{\mu}_1) \cdot u(x_2, \hat{\mu}_2) \ldots u(x_f, \hat{\mu}_f)\right], \tag{2.10a}$$

with the convention $-\frac{1}{2} < q_\mathrm{F} < \frac{1}{2}$. In terms of phases we get

$$2\pi q_\mathrm{F}(\mathrm{S}) = \sum_{i=1}^{f} \phi(x_i, \hat{\mu}_i) + 2\pi K(\mathrm{S}), \tag{2.10b}$$

where the integer $K(\mathrm{S})$ is defined such that $-\frac{1}{2} < q_\mathrm{F} < \frac{1}{2}$ holds. $q_\mathrm{F}(\mathrm{S})$ is gauge invariant, in particular also under gauge transformations which are singular at a centre of some plaquette.

* Exceptional configurations $\phi = \pm\pi$ are excluded.

By taking boundaries of appropriate triangles the definitions (2.5) and (2.7) are reobtained. For the square lattice we add a third definition by taking S to be the boundary ∂p of the plaquette p:

$$q_3(\mathrm{p}) := q_{\mathrm{F}}(\partial \mathrm{p}) = \frac{1}{2\pi} \sum_{i=1}^{4} \phi(x_i, \hat{\mu}_i) + K(\partial \mathrm{p}). \tag{2.11}$$

It is easy to show that eq. (2.8) remains valid.

3. Universal topological charge

3.1. SCALING BEHAVIOUR AND DISLOCATIONS

Let us consider a model with asymptotic scaling behaviour

$$\xi = a \,\mathrm{const}\, \beta^P \exp(\tfrac{1}{2}\alpha\beta)\left(1 + \mathrm{O}\left(\frac{1}{\beta}\right)\right), \qquad \beta \to \infty, \tag{3.1}$$

for the correlation length ξ. This means a physical mass^2, like the topological susceptibility, is expected to scale like $\beta^{-2P}\exp(-\alpha\beta), \beta \to \infty$ (see also [13]).

Let $\delta > 0$ be fixed. By a *dislocation* D_δ we understand a lattice spin configuration with the following properties:

(a) A set A_δ of link-wise connected plaquettes exists such that

(i) each plaquette $\mathrm{p} \in \mathrm{A}_\delta$ contains at least one interior link ℓ ("interior" with respect to A_δ) with action $S_\ell > \delta$;

(ii) for links ℓ from the boundary $\partial \mathrm{A}_\delta$ we have $S_\ell > \delta$.

The set A_δ will be called the *dislocation region* in the following.

(b) A constant spin s ($s^2 = 1$) exists such that if we set all spins s_i, which are not attached to plaquettes $\mathrm{p} \in \mathrm{A}_\delta$, equal to $s_i = s$, the configuration thus obtained has

(i) $S_\ell < \delta$ for all links $\ell \notin \mathrm{A}_\delta$,

(ii) topological charge $|Q| \neq 0$.

(Definitions of the CP^1 topological charge are as in the previous section and for the CP^N ($N \geqslant 2$) model as in ref. [3].)

Let S_0 be the smallest action of such a dislocation. Our model is supposed to have classical instanton solutions and consequently

$$S_{\mathrm{D}} := \lim_{\delta \to 0} S_{\mathrm{D}}^{\delta} \leqslant S_{\mathrm{inst}} \tag{3.2}$$

holds, where S_{inst} is the continuum one-instanton action and S_{D} is, in the $|Q| \neq 0$ sectors, the minimal action on an infinite lattice. For the O(3) σ-model S_{D} is given by eq. (1.5) and

$$S_{\mathrm{inst}} = 4\pi \text{ (ref. [4])}. \tag{3.3}$$

Relying on partition function (2.2), the probability that for β large (δ fixed) a dislocation, containing a particular plaquette p_0 of the lattice, occurs is proportional to $\beta^{P'}e^{-\beta S_{\mathrm{D}}^{\delta}}$. This gives rise to a dilute gas of dislocations, contributing according to eq. (1.6) to the topological susceptibility. Assuming the scaling behaviour (3.1), this implies: dislocations are harmless if

$$S_{\mathrm{D}} > \alpha, \tag{3.4a}$$

but dislocations will overwhelm the physical long-range fluctuations if

$$S_{\mathrm{D}} < \alpha. \tag{3.4b}$$

Dislocations are non-universal as is seen easily by studying the modified partition function

$$Z_{\varepsilon} = \int \prod_{j} \mathrm{d}s_j \prod_{\ell} \theta(\varepsilon - S_{\ell}) e^{-\beta S}. \tag{3.5}$$

The product $\prod_{\ell}$ is over all links of the lattice. Z of eq. (2.2) is obtained by setting $\varepsilon = 2$. The minimal $|Q| \neq 0$ action is now

$$S_{\mathrm{D}}(\varepsilon) = \lim_{\delta \to 0} S_{\mathrm{D}}^{\delta}(\varepsilon), \tag{3.6}$$

and one recognizes

$$\lim_{\varepsilon \to 0} S_{\mathrm{D}}(\varepsilon) = S_{\mathrm{inst}}. \tag{3.7}$$

In case of the CP^1 model this means $S_{\mathrm{D}}(\varepsilon)$ has to increase from 6.69 to 4π, when ε varies from 2 down to 0.

For the CP^N models one has $\alpha = 8\pi/(N+1)$ and $S_{\mathrm{inst}} = 4\pi$, implying that a *value* ε_{c} exists, such that dislocations become harmless for $\varepsilon < \varepsilon_{\mathrm{c}}$. Lüscher [7] has shown that for $N \geqslant 3$ this is already the case with the standard action. The CP^1 model is a special case, because $\alpha = S_{\mathrm{inst}} = 4\pi$. Consequently the physical result* χ_{t} for the topological susceptibility is obtained in the limit

$$\chi_{\mathrm{t}} = \lim_{\varepsilon \to 0} \lim_{\beta \to \infty} \lim_{V \to \infty} \chi_{\mathrm{t}}(\varepsilon, \beta, V). \tag{3.8}$$

In contrast any choice $\varepsilon < \varepsilon_{\mathrm{c}}$ is sufficient for the CP^2 model. To exhibit the order of limits we have also included the volume V and coupling constant β dependence in eq. (3.8).

* Ignoring the ultraviolet problem.

3.2. TOPOLOGICAL CHARGE

Instead of relying on particular actions, we like to incorporate the considerations of the previous subsection into the definition of the topological charge. Otherwise the concept of universality is obscured. In fact the authors of ref. [14] take the original definition [3] of the topological charge more seriously than universality and suggest new universality classes. In view of our results we see, however, no reason for introducing such radical innovations.

The new charge

$$Q_{\mathrm{B}}^{\delta} = Q - Q_{\mathrm{D}}^{\delta} \qquad (\delta > 0 \text{ “cut-off” parameter}) \tag{3.9}$$

is constructed [11] to give identical physical results on all actions of the whole universality class. The physical topological susceptibility χ_{B}, defined by

$$\chi_{\mathrm{B}} = \lim_{\delta \to 0} \lim_{\beta \to 0} \lim_{V \to \infty} \frac{1}{V} \langle (Q_{\mathrm{B}}^{\delta})^2 \rangle \tag{3.10}$$

is supposed to scale according to

$$\chi_{\mathrm{B}} = a^{-2} \mathrm{const}_{\mathrm{B}} \beta^{-2P} \exp(-\alpha\beta) \left(1 + \mathrm{O}\left(\frac{1}{\beta}\right)\right), \qquad \beta \to \infty, \tag{3.11}$$

and for different actions the different $\mathrm{const}_{\mathrm{B}}$ are related by perturbative Λ-parameter calculations.

The physical background charge Q_{B}^{δ} is defined by subtracting from the old charge Q the charge Q_{D}^{δ} of dislocations with $S_{\mathrm{l}} > \delta$ at at least one link ℓ. The precise definition of Q_{D}^{δ} is

$$Q_{\mathrm{D}}^{\delta} = \sum_{\mathrm{A}_{\delta}} \left\{ \sum_{\mathrm{p} \in \mathrm{A}_{\delta}} q(\mathrm{p}) - q_{\mathrm{F}}(\partial \mathrm{A}_{\delta}) \right\}. \tag{3.12}$$

Here the first sum goes over all dislocation regions as introduced in the previous subsection. $q(\mathrm{p})$ stands for one of the definitions (2.5), (2.7) or (2.11), $q_{\mathrm{F}}(\mathrm{S})$ is defined by (2.10) and $\mathrm{S} = \partial \mathrm{A}_{\delta}$ is the boundary of A_{δ}.

Examples of dislocation regions are depicted in fig. 2. Let p_0 be a particular plaquette of the lattice. For δ fixed, $\beta \to \infty$ the probability $P(\mathrm{A}_{\delta})$ of finding a region $\mathrm{A}_{\delta} \ni \mathrm{p}_0$ on the lattice is estimated by

$$P(\mathrm{A}_{\delta}) < \mathrm{const}\, \beta^{P''} \mathrm{e}^{-n\beta\delta}. \tag{3.13}$$

Here n is the number of *interior* links $\ell \in \mathrm{A}_{\delta}$. For β large typical dislocations

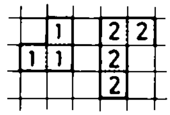

Fig. 2. Three examples of dislocation regions which would contribute in (3.12). Links with $S_\ell > \delta$ are dotted.

regions are small. Properties of the topological charge Q_{B}^{δ} ($\delta > 0$ fixed) are:

(i) Q_{B}^{δ} sums up from a (quasi) *local* charge density. Putting together eqs. (3.9) and (3.12), we find

$$Q_{\mathrm{B}}^{\delta} = \sum_{\substack{\mathrm{p} \\ \mathrm{p} \notin U \mathrm{A}_\delta}} q(\mathrm{p}) + \sum_{\mathrm{A}_\delta} q_{\mathrm{F}}(\partial \mathrm{A}_\delta) . \tag{3.14}$$

In the continuum limit, all dislocation regions A_δ, contributing to (3.14) have area zero. We call this property (quasi) locality.

Proof: Let G be a region of fixed physical size, i.e. fixed in units $[\xi]$ of the correlation length. Then the number of plaquettes inside G increases proportionally to $\beta^{2P}\exp(\alpha\beta)$, $\beta \to \infty$. Therefore, the probability (3.13) of finding inside G a dislocation region A with n interior links goes to zero if $n > \alpha/\delta$. On the other hand, for possible A_δ

$$n \leqslant \frac{\alpha}{\delta} \tag{3.15}$$

holds. Consequently the area of any A_δ, contributing to Q_{B}^{δ}, goes to zero in the continuum limit.

(ii) Q_{B}^{δ} takes integer values $0, \pm 1, \dots$.
This follows immediately from eqs. (3.14) and (2.10b).

(iii) $Q_{\mathrm{B}}^{\delta} = 0$ for a dislocation D_δ (as defined in subsect. 3.1). This is of course the most important property.

Proof: For small δ all boundary spins of A_δ are in the same half-sphere as the fixed spin s. Eqs. (3.14) and $-\frac{1}{2} < q_{\mathrm{F}}(\partial \mathrm{A}_\delta) < \frac{1}{2}$(2.10) imply $Q_{\mathrm{B}}^{\delta} = 0$.

(iv) $q_{\mathrm{F}}(\partial \mathrm{A}_\delta) \neq \Sigma_{\mathrm{p} \in \mathrm{A}_\delta} q(\mathrm{p})$ if and only if $|\Sigma_{\mathrm{p} \in \mathrm{A}_\delta} q(\mathrm{p})| > \frac{1}{2}$. This shows how unphysical contributions ($|\Sigma q(\mathrm{p})| > \frac{1}{2}$ from a region of area 0) are now suppressed. Remember: $|q_{\mathrm{F}}(\partial \mathrm{A}_\delta)| < \frac{1}{2}$ always.

(v) Conjecture: Assume an ε_{c} (as defined after (3.7)) exists, then

$$0 < \delta_1, \delta_2 < \varepsilon_{\mathrm{c}} \tag{3.16a}$$

implies

$$\lim_{\beta \to \infty} \lim_{V \to \infty} \chi_{\mathrm{B}}^{\delta_1}(\beta, V) = \lim_{\beta \to \infty} \lim_{V \to \infty} \chi_{\mathrm{B}}^{\delta_2}(\beta, V) . \tag{3.16b}$$

The conjecture is plausible but difficult to prove, because the continuum limit is involved.

Remarks:

(i) Q_{B}^{δ} is defined up to exceptional configurations. For δ small enough ($\delta < \varepsilon^{\Delta}$, $\varepsilon^{\Box}$ see (2.6), (2.8)) exceptional configurations are those for which $q_{\mathrm{F}}(\partial \mathrm{A}_{\delta})$ (at one or more A_{δ}) is not defined (this means $q_{\mathrm{F}}(\partial \mathrm{A}_{\delta}) = \pm \frac{1}{2}$). Q_{B}^{δ} may be well defined by (3.14), although the dislocation charge Q_{D}^{δ} (3.12) is not defined.

(ii) The O(3) σ-model is a particularly bad case, because $\varepsilon_{\mathrm{c}} = 0$ and therefore the limit $\delta \to 0$ in the definition of χ_{B} (3.10) has, in principle, to be carried out. In practice finite δ may, however, already give reasonable results, as is indicated by the existence of quasistable configurations [6] of topological charge $|Q| \neq 0$. In view of the computational simplicity of the O(3) model and our limited computer time, we decided to carry out a MC simulation for this model.

4. Numerical results

Let us first describe the computer implementation of the topological charge Q_{B} (3.14). For all links ℓ and all plaquettes p of the lattice logical variables $L(\ell)$ and $P(\mathrm{p})$ are introduced. Initially all these variables are set equal to F = "false". Then we scan through all links ℓ of the lattice and set $P(\mathrm{p}_i) = \mathrm{T} =$ "true" $(i = 1, 2)$ for the two neighbour plaquettes of any link ℓ with $S_{\ell} > \delta$. After, in this way, all $P(\mathrm{p})$ have been assigned to their final values, we scan again through all links of the lattice and put

$$L(\ell) = T \quad \text{if} \quad \boxed{\begin{array}{c} \mathrm{T} \\ -\ell- \\ \mathrm{F} \end{array}} \quad \text{or} \quad \boxed{\begin{array}{c} \mathrm{F} \\ -\ell- \\ \mathrm{T} \end{array}}$$

happens with respect to the logical variables of the two neighbour plaquettes*. Otherwise the value $L(\ell) = \mathrm{F}$ is kept. In that way the $P(\mathrm{p}) = \mathrm{T}$ plaquettes are inside dislocation regions A_{δ} and $L(\ell) = \mathrm{T}$ links define boundaries of dislocation regions A_{δ}. The computation of the boundary contributions $q_{\mathrm{F}}(\partial \mathrm{A}_{\delta})$ to the topological charge proceeds now in the following way.

We make a loop over all links ℓ.

(i) if $L(\ell) = \mathrm{F}$ we go immediately to link $\ell + 1$.

(ii) If $L(\ell) = \mathrm{T}$ we compute (using the CP^1 language) the contribution of this link ℓ to $q_{\mathrm{F}}(\partial \mathrm{A}_{\delta})$. Then we set $L(\ell) = \mathrm{F}$ and search in anti-clockwise direction for a new link ℓ' (which exists) with $L(\ell') = \mathrm{T}$. We proceed until we hit the starting point of link ℓ. Then we go on like as before (i) with link $\ell + 1$.

* The plaquettes may be triangles.

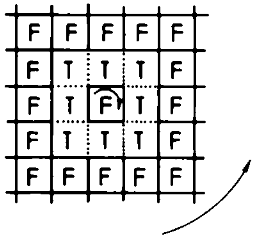

Fig. 3. A dislocation region, which requires special care. Links with $S_\ell > \delta$ are dotted. The boundary contributions to the charge are taken with orientations as indicated by the arrows.

Special care is taken to exclude configurations which are closed by cyclic boundary conditions, and to treat correctly configurations as shown in fig. 3. MC results are obtained on square and on triangular lattices.

4.1. SQUARE LATTICE

We work on a 100×100 lattice. A sweep is defined by upgrading each spin on the lattice once in the mean. We use random upgrading. Our final statistics are obvious from table 1.

In table 2 our results for the mean action per link $\langle S_\ell \rangle$, for the magnetic susceptibility

$$\chi_m = \frac{1}{V}\left\langle \left(\sum_i s_i\right)^2 \right\rangle, \tag{4.1}$$

and for the magnetic defect

$$\delta_m := 2 \cdot 10^5 \beta^4 e^{-4\pi\beta} \chi_m \tag{4.2}$$

TABLE 1

100×100 square lattice:
$N_{\text{equil.}}$ = no. of sweeps for equilibrium, $N_{\text{multiplicity}}$ = no. of sweeps before each measurement, $N_{\text{measurements}}$ = no. of measurements

β	$N_{\text{equil.}}$	$N_{\text{multiplicity}}$	$N_{\text{measurements}}$
1.4	7231	5	1500
1.5	8138	5	1671
1.6	7176	5	3261
1.65	9215	10	3254
1.7	8212	10	9050
1.75	9149	10	3985
1.8	8000	10	7534
1.85	9692	20	4683
1.9	8636	25	4382

TABLE 2
100×100 square lattice:
average action per link $\langle S_\ell \rangle$, magnetic susceptibility χ_m and magnetic defect δ_m

β	$\langle S_\ell \rangle$	χ_m	δ_m
1.40	0.438	67 ± 7	1.17 ± 0.12
1.50	0.398	151 ± 20	1.00 ± 0.13
1.60	0.365	325 ± 69	0.79 ± 0.17
1.65	0.349	755 ± 76	1.11 ± 0.11
1.70	0.336	964 ± 70	0.85 ± 0.07
1.75	0.3230	1577 ± 47	0.816 ± 0.024
1.80	0.3117	1822 ± 74	0.574 ± 0.023
1.85	0.3016	1937 ± 88	0.363 ± 0.016
1.90	0.2920	2183 ± 47	0.243 ± 0.005

are collected. Within statistical errors the data are consistent with old results [15, 3]. Scaling of the magnetic susceptibility looks better than before.

Measurements of the topological charge Q_B^δ first require preliminary investigations about reasonable values for the cut-off parameters δ. Our calculation of Q_B^δ breaks down if, on the average, more than about 30% of the plaquettes get "true" assigned. We decided to first make histograms of the action per link distribution.

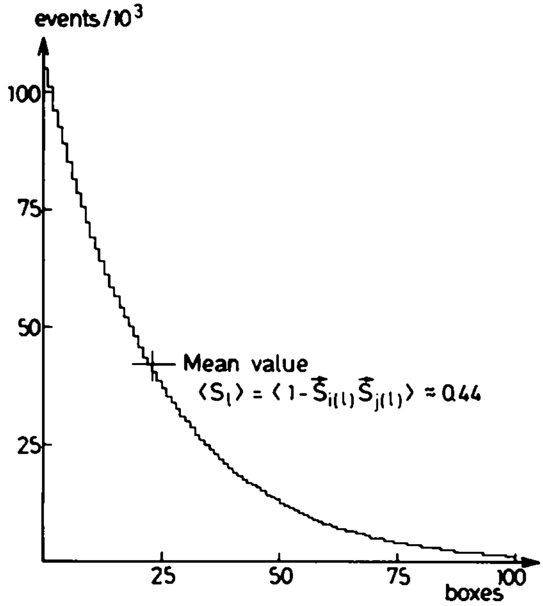

Fig. 4. Histogram of the action per link distribution at $\beta = 1.4$. In the horizontal axis there are 100 boxes covering the range $0 \leqslant \langle S_\ell \rangle \leqslant 2$. The vertical axis gives the number of events. (500 sweeps on a 50^2 lattice: total number of events $2.5 \cdot 10^6$.)

TABLE 3
100 × 100 square lattice:
percentage of "true" plaquettes for different cut-offs δ

$\beta \backslash \delta$	0.7	0.8	0.9	1.0	1.1	1.2	1.3	1.4	1.5
1.40					24.8	19.7	15.4	11.8	8.8
1.50				24.8	19.4	14.9	11.3	8.3	6.0
1.60			25.9	19.8	15.0	11.1	8.1	5.8	4.0
1.65			23.3	17.6	13.1	9.5	6.8	4.8	3.3
1.70		28.0	21.2	15.7	11.5	8.2	5.8	4.0	2.7
1.75		25.7	19.1	14.0	10.0	7.1	4.9	3.3	2.2
1.80		23.7	17.3	12.5	8.8	6.1	4.2	2.8	1.8
1.85		21.9	15.8	11.2	7.8	5.3	3.6	2.3	1.5
1.90	27.8	20.1	14.3	10.0	6.8	4.6	3.0	1.9	1.2

For $\beta = 1.4$ an example is given in fig. 4. The finally used cut-offs are collected in table 3. In the region up to $\beta = 1.9$ the lowest possible cut-off is $\delta = 0.7$. Otherwise too many plaquettes become "true" assigned.

For the topological charge density at a single plaquette we use three different definitions $q_i(\mathrm{p})$ ($i = 1,2,3$), see eqs. (2.7) and (2.11). Dislocations for which the $q_i(\mathrm{p})$ differ at a plaquette are called 1-plaquette dislocations in [6]. From table 4 we recognize that for $\delta \leqslant 1.0$ all three definitions of Q_{B}^{δ} agree. This is a consequence of eq. (2.8). Already with the cut-off values $\delta = 1.1$ and $\delta = 1.2$ we find from table 4 a strong suppression of the 1-plaquette dislocations.

In the cut-off region $\delta \leqslant 1.3$ the obtained values $\langle (Q_{\mathrm{B}_i}^{\delta})^2 \rangle$ are nearly identical for $i = 1,2,3$. For larger cut-offs the $\langle (Q_{\mathrm{B}_3}^{\delta})^2 \rangle$ values are lower than the $\langle (Q_{\mathrm{B}_i}^{\delta})^2 \rangle$

TABLE 4
Agreement of the different definitions of the topological charge Q_{B}

$\beta \backslash \delta$	0.7	0.8	0.9	1.0	1.1	1.2	1.3	1.4	1.5
1.40					97.7%	76.1%	38%	16%	5%
1.50				100%	99.1%	86.6%	58%	29%	13%
1.60			100%	100%	99.4%	93.0%	75%	51%	29%
1.65			100%	100%	99.6%	94.9%	83%	63%	42%
1.70		100%	100%	100%	99.7%	96.4%	87%	71%	53%
1.75		100%	100%	100%	99.8%	97.6%	91%	80%	65%
1.80		100%	100%	100%	99.8%	98.3%	93.4%	85%	75%
1.85		100%	100%	100%	99.9%	98.9%	95.7%	90%	81%
1.90	100%	100%	100%	100%	99.9%	98.9%	96.5%	92.6%	86%

($i = 1, 2$) values. To be definite, we now use

$$\left\langle \left(Q_{\mathrm{B}}^{\delta}\right)^2 \right\rangle = \tfrac{1}{2}\left(\left\langle \left(Q_{\mathrm{B}_1}^{\delta}\right)^2 \right\rangle + \left\langle \left(Q_{\mathrm{B}_2}^{\delta}\right)^2 \right\rangle\right). \tag{4.3}$$

As in ref. [3] we define the topological defect by

$$\delta_t^{\delta} = 10^{-5}\beta^{-2}e^{+4\pi\beta}\frac{\left\langle \left(Q_{\mathrm{B}}^{\delta}\right)^2 \right\rangle}{V}. \tag{4.4}$$

Our MC data for the defect are collected in table 5. In the region $\beta \geqslant 1.6$ the values obtained with low cut-offs are consistent with scaling. Fig. 5 summarizes the relevant results. The improvement from $\delta = 2.0$ (no cut-off) down to the nearly flat results for $\delta = 0.9, 0.8, 0.7$ is rather impressive.

Finally, in this subsection, table 6 gives the percentage of $Q_{\mathrm{B}} = 0$ configurations for different couplings and low ($\delta \leqslant 1.0$) cut-offs. For β large tunneling becomes important and slows down the convergence considerably. See also the subsect. 4.2.

TABLE 5
100×100 square lattice: topological defect δ_t

β	$\delta = 0.7$	$\delta = 0.8$	$\delta = 0.9$	$\delta = 1.0$	$\delta = 1.1$
1.40					0.269 (6)
1.50				0.429 (16)	0.475 (25)
1.60			0.708 (17)	0.767 (25)	0.862 (35)
1.65			0.727 (53)	0.811 (51)	0.897 (45)
1.70		0.810 (40)	0.894 (37)	0.974 (39)	1.091 (42)
1.75		0.697 (42)	0.798 (49)	0.907 (60)	1.025 (70)
1.80		0.639 (53)	0.743 (52)	0.864 (61)	0.991 (50)
1.85		1.103 (177)	1.232 (169)	1.339 (177)	1.505 (188)
1.90	0.902 (107)	0.962 (137)	1.129 (131)	1.241 (122)	1.386 (140)
β	$\delta = 1.2$	$\delta = 1.3$	$\delta = 1.4$	$\delta = 1.5$	$\delta = 2.0$
1.40	0.317 (6)	0.376 (10)	0.445 (9)	0.445 (18)	0.920 (34)
1.50	0.528 (25)	0.609 (33)	0.707 (23)	0.813 (32)	1.561 (56)
1.60	0.966 (36)	1.085 (45)	1.222 (49)	1.368 (49)	2.670 (63)
1.65	1.013 (48)	1.126 (52)	1.304 (53)	1.470 (57)	2.961 (83)
1.70	1.226 (49)	1.376 (52)	1.594 (55)	1.859 (57)	3.813 (69)
1.75	1.175 (71)	1.382 (80)	1.596 (89)	1.922 (94)	4.233 (137)
1.80	1.168 (52)	1.380 (62)	1.708 (63)	2.067 (66)	5.147 (136)
1.85	1.683 (196)	1.943 (207)	2.296 (198)	2.667 (207)	6.65 (20)
1.90	1.656 (155)	2.030 (153)	2.425 (171)	2.961 (188)	7.48 (22)

The number in brackets gives the expected error in the last digits.

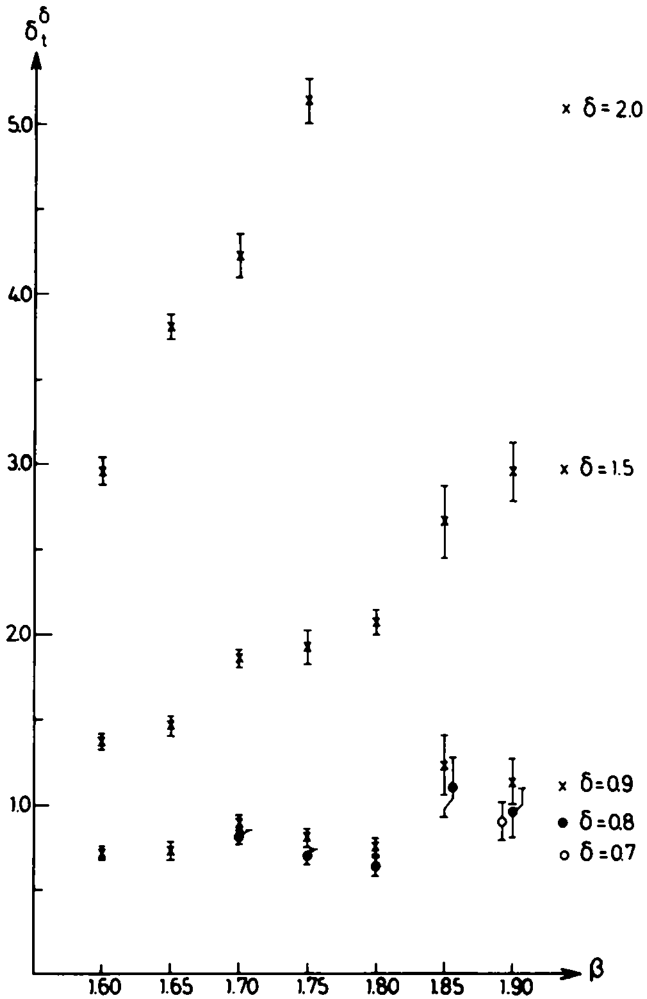

Fig. 5. 100 × 100 square lattice: topological defect.

TABLE 6
100 × 100 square lattice: percentage of $Q_B^\delta = 0$ configurations

β	$\varepsilon = 0.7$	$\varepsilon = 0.8$	$\varepsilon = 0.9$	$\varepsilon = 1.0$
1.50				16
1.60			21	20
1.65			31	29
1.70		40	38	37
1.75		61	57	54
1.80		75	71	68
1.85		75	73	71
1.90	88	87	85	83

TABLE 7
100 × 100 triangular lattice:
N_{equil} = no. of sweeps for equilibrium, $N_{\mathrm{multiplicity}}$ = no. of sweeps before each measurement, $N_{\mathrm{measurements}}$ = no. of measurements

β	$N_{\mathrm{equil.}}$	$N_{\mathrm{multiplicity}}$	$N_{\mathrm{measurements}}$
0.8	7040	10	1488
0.9	6846	15	936
1.0	7382	15	3213
1.1	7522	15	4480
1.2	7514	25	4568
1.3	7506	25	4024

4.2. TRIANGULAR LATTICE

We work on an (approximately square) 100×116 lattice (see sect. 2 for the notation). Our final statistics are summarized in table 7.

Table 8 collects our results for the mean action per link $\langle S_{\ell} \rangle$, for the magnetic susceptibility χ_{m} (4.1), and the magnetic defect, now defined by

$$\delta_{\mathrm{m}} := 2 \cdot 10^{5} \left(\tfrac{3}{2}\beta\right)^{4} \mathrm{e}^{-4\pi(3/2)\beta} \chi_{\mathrm{m}} . \tag{4.5}$$

For the topological charge Q_{B}^{δ} we again consider cut-offs in the range $0.7 \leqslant \delta \leqslant 1.5$. The topological defect is now defined by

$$\delta_{\mathrm{t}} := 10^{-5} \left(\tfrac{3}{2}\beta\right)^{-2} \mathrm{e}^{+4\pi(3/2)\beta} \frac{\langle (Q_{\mathrm{B}})^{2} \rangle}{V} , \tag{4.6}$$

and our MC data for the defect are given in table 9. Fig. 6 exhibits relevant results for different cut-offs δ. We see that the $\delta = 1.0$ results are nearly flat (albeit still lowered by taking even smaller values δ), and even the $\delta = 1.5$ data look quite reasonable. In comparison, results with $\delta = 2.0$ (no cut-off) do not indicate scaling at

TABLE 8
100 × 116 triangular lattice:
average action per link $\langle S_{\ell} \rangle$, magnetic susceptibility χ_{m} and magnetic defect δ_{m}

β	$\langle S_{\ell} \rangle$	χ_{m}	δ_{m}
0.8	0.529	42 ± 3	4.96 ± 0.25
0.9	0.453	154 ± 17	4.38 ± 0.48
1.0	0.390	749 ± 85	4.94 ± 0.56
1.1	0.344	1935 ± 92	2.84 ± 0.14
1.2	0.309	2867 ± 87	0.90 ± 0.03
1.3	0.281	3623 ± 56	0.24 ± 0.01

TABLE 9
100×116 triangular lattice: topological defect δ_t^δ

β	$\delta = 0.7$	$\delta = 0.8$	$\delta = 0.9$	$\delta = 1.0$	$\delta = 1.1$
0.8					0.053 (2)
0.9				0.129 (6)	0.148 (8)
1.0		0.159 (8)	0.179 (8)	0.199 (9)	0.216 (10)
1.1	0.116 (13)	0.129 (12)	0.153 (13)	0.175 (16)	0.201 (16)
1.2	0.182 (100)	0.200 (98)	0.222 (94)	0.250 (94)	0.280 (93)
1.3	0.068 (19)	0.074 (13)	0.115 (22)	0.152 (18)	0.198 (18)

β	$\delta = 1.2$	$\delta = 1.3$	$\delta = 1.4$	$\delta = 1.5$	$\delta = 2.0$
0.8	0.061 (3)	0.070 (2)	0.082 (2)	0.094 (3)	0.186 (6)
0.9	0.166 (8)	0.176 (10)	0.200 (9)	0.214 (10)	0.458 (28)
1.0	0.240 (11)	0.270 (12)	0.303 (9)	0.347 (7)	0.826 (24)
1.1	0.232 (16)	0.268 (16)	0.312 (16)	0.370 (16)	1.24 (4)
1.2	0.320 (98)	0.350 (96)	0.413 (90)	0.502 (89)	2.00 (8)
1.3	0.227 (21)	0.287 (27)	0.356 (28)	0.450 (33)	3.17 (13)

The number in brackets gives the expected error in the last digits.

all. Crude estimates for the defects are

$$\delta_t^{\square} \lesssim 0.95 \qquad \text{(square lattice)}, \tag{4.7a}$$

$$\delta_t^{\Delta} \lesssim 0.40 \qquad \text{(triangular lattice)}. \tag{4.7b}$$

This gives the MC estimate

$$\Lambda_L^{\Delta} \approx 1.5\Lambda_L^{\square} \tag{4.8a}$$

for the Λ-scales. In comparison, the perturbative result [12] is

$$\Lambda_L^{\Delta} = 1.04\Lambda_L^{\square}. \tag{4.8b}$$

In view of possible large systematical and statistical uncertainties in eqs. (4.7), the order of disagreement is not unexpected. Furthermore, we note that a different MC estimate, $\Lambda_L^{\Delta} \approx 0.5\Lambda_L^{\square}$, is obtained by comparing the magnetic defects in their flat region.

We obtain a better consistency if we take the product $\chi_t\chi_m$ in a region of couplings where both χ_t and χ_m scale approximately. Using a cut-off $\delta = 1.0$, we find

$$10^{-3}\chi_t\chi_m(\beta = 1.65) \approx 1766 \pm 120 \qquad \text{(square)},$$

$$10^{-3}\chi_t\chi_m(\beta = 1.0) \approx 1997 \pm 180 \qquad \text{(triangular)}.$$

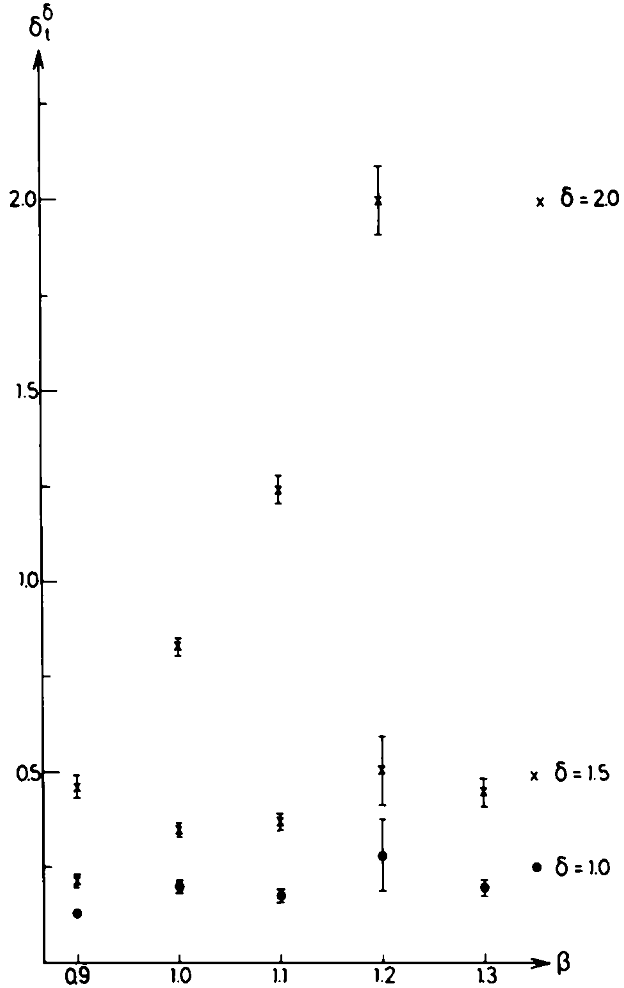

Fig. 6. 100 × 116 triangular lattice: topological defect.

We remark that $\chi_t \chi_m$ (in contrast to $\xi^2 \chi_t$) still has perturbative $1/\beta$ corrections to scaling. Somewhat disturbing in fig. 6 are the large error bars at $\beta = 1.2$, as compared with $\beta = 1.1$ and $\beta = 1.3$. It is due to a rare tunneling event which kept the simulation for quite a while in a rather stable $|Q_B| \neq 0$ sector. This signals that other error bars, in particular at $\beta = 1.2$, may be unreliable. From table 10 we read off that at $\beta = 1.9$ nearly all generated configurations were in the charge $Q_B = 0$ sector. To increase the tunneling speed between different sectors an interesting suggestion [16] is to offer, from time to time, instanton and anti-instanton rotations around a fixed spin. Properly implemented, such a procedure does not destroy detailed balance.

TABLE 10
100 × 116 triangular lattice: percentage of $Q_B^\delta = 0$ configurations

β	$\delta = 0.7$	$\delta = 0.8$	$\delta = 0.9$	$\delta = 1.0$	$\delta = 1.1$	$\delta = 1.2$	$\delta = 1.3$	$\delta = 1.4$	$\delta = 1.5$
0.8					9	9	8	7	7
0.9				13	12	11	12	10	10
1.0		28	26	24	24	22	20	19	19
1.1	75	72	69	66	62	58	54	50	45
1.2	92	91	90	89	87	86	84	82	79
1.3	99	99	99	99	98	98	97	97	96

5. Conclusions

Following a previous suggestion [11], we succeeded in defining the lattice topological charge for all actions of the whole universality class. Numerical results are encouraging. It would be interesting to repeat similar calculations for the CP^2 model. Using the standard action and our background charge Q_B, we expect for the universal quantity

$$\xi^2 \chi_B \tag{5.1}$$

(ξ is correlation length, χ_B topological susceptibility) consistency with results previously obtained by Petcher and Lüscher [12]. Also, modified CP^2 actions allow one to test the conjecture (3.16) numerically.

Finally, we remark that the problem treated is also of importance for 4d non-abelian gauge theories. Even if the dislocation problem does not exist for the standard action, other actions in the same universality class will have it. Again, our construction is needed to ensure a manifest formulation of universality for the topological susceptibility.

We would like to thank the DESY computer center for providing the necessary CPU time. One of the authors (C.P.) would like to acknowledge the kind hospitality of F. Gutbrod and the DESY theory group.

References

[1] P. di Vecchia, Acta Phys. Austr., Suppl. XXII (1980) 341 (Schladming lectures 1980)
[2] P. Collela and O.E. Lanford, in Constructive quantum field theory, ed. G. Velo and A. Wightman, Lecture notes in physics, vol. 25, (Springer, 1973)
[3] B. Berg and M. Lüscher, Nucl. Phys. B190[FS3] (1981) 412
[4] A.A. Belavin and A.M. Polyakov, JETP Lett. 2 (1975) 245
[5] V.A. Fateev, I.V. Frolov and A.S. Schwarz, Nucl. Phys. B154 (1979) 1;
B. Berg and M. Lüscher, Commun. Math. Phys. 69 (1979) 57
[6] B. Berg, Phys. Lett. 104B (1981) 475

[7] M. Lüscher, Nucl. Phys. B200[FS4] (1982) 61
[8] G. Martinelli, R. Petronzio and M.A. Virasoro, Nucl. Phys. B205[FS5] (1982) 355
[9] J. Kogut and K. Wilson, Phys. Reports 12 (1974) 75
[10] M. Lüscher, unpublished
[11] B. Berg, in Proc. Int. Conf. on High energy physics, ed. J. Dias de Deus and J. Soffer (European Physical Society, 1982) p. 1033 ff.
[12] D. Petcher and M. Lüscher, Nucl. Phys. B225[FS9] (1983) 53
[13] M. Evans, Nucl. Phys. B208 (1982) 122
[14] Y. Iwasaki and T. Yoshie, Phys. Lett. 125B (1983) 201
[15] G. Martinelli, G. Parisi and R. Petronzio, Phys. Lett. 100B (1981) 485
[16] F. Fucito and S. Solomon, Phys. Lett. 134B (1984) 230